Two Magnon Scattering Contribution to the Ferromagnetic Resonance Linewidth of Pt(Ir)/CoFeTaB/Ir(Pt) thin films

M. Tokaç,[1] S. Kazan,[2,*] B. Özkal,[2] N. Al-jawfi,[2] B. Rameev,[2,3,4] B. Nicholson,[5] and A.T. Hindmarch[5]

[1]*Department of Fundamental Sciences, Faculty of Engineering, Alanya Alaaddin Keykubat University, 07450, Antalya, Türkiye*
[2]*Department of Physics, Gebze Technical University, 41400, Kocaeli, Türkiye*
[3]*Kazan State Power Engineering University, 420066, Kazan, Tatarstan, Russian Federation*
[4]*Zavoisky Physical-Technical Institute, FRC Kazan Scientific Center of Russian Academy of Sciences, 420029, Kazan, Tatarstan, Russian Federation*
[5]*Department of Physics, Durham University, South Road, Durham, DH1 3LE, United Kingdom*

The magnetic properties of Pt/CoFeTaB/Ir and Ir/CoFeTaB/Pt trilayer thin films have been studied using angular- and temperature-dependent ferromagnetic resonance. This enables quantitative determination of the various contributions to the magnetic behavior, including separating the effective Gilbert damping, inhomogeneous damping, and two-magnon-scattering contributions to the magnetic dissipation. As-deposited films show behavior consistent with significant incorporation of Ir into CoFeTaB only when the Ir layer is deposited first. Annealing of the structures at 300°C causes only minor structural and magnetic modification when Pt is deposited first, and more pronounced changes, attributed to thermally-driven out-diffusion of Ir from CoFeTaB, are found when Ir is deposited first. A holistic consideration of the magnetic resonance behavior can provide detailed information on the atomic-scale structure in magnetic thin-film devices.

INTRODUCTION

Heavy metal/ferromagnetic (HM/FM) structures have been extensively studied for their use in interface-driven spintronics applications [1–7] where the HM/FM interface can give rise to a variety of magnetic phenomena, such as spin pumping [2–4], spin Hall magnetoresistance [5, 6], spin Seebeck effect [8], interfacial Dzyaloshinskii-Moriya interaction [9, 10] and spin-mixing conductance [11, 12]. In addition to the strength of spin-orbit coupling and the broken inversion symmetry at the HM/FM interface, the sign and magnitude of the antisymmetric exchange interaction, the so-called interfacial Dzyaloshinskii–Moriya interaction, are directly correlated to the degree of interfacial 3d-5d hybridization around the Fermi level [13]. The DMI gives rise to a rich variety of chiral magnetic textures in thin magnetic films, which show promise in future spintronic applications due to their unique properties. Experimental studies have shown that the magnitude and the sign of the interfacial DMI in multilayers depend on the types of HM and FM layers [14], the thickness of the HM layer [15], and atomic inter-diffusion at the HM/FM interface [16]. The underlying physics of the interfacial DMI is still not fully understood, despite its technological importance and extensive studies, hence offers unique opportunities to elucidate the underlying physical origin of the interfacial DMI.

Electronic hybridization between the FM and HM layers can exhibit proximity-induced-magnetization (PIM), where spontaneous magnetic polarization arises in the interfacial region [17]. A number of studies have been conducted on the significance of PIM on the spin transport mechanism across the HM/FM interface to understand the role of PIM contribution to the improvement of Gilbert damping [18–20] where thin Pt and/or Ir layers are used in most studies due to their large spin-orbit coupling. However, the role of the PIM is still unclear. Hybridization at the HM/FM interface has been shown to be both a primary factor in [21], and unimportant to [22], controlling the strength of DMI. Ferromagnetic resonance (FMR) has shown that a decrease in PIM correlated with a decreased interfacial contribution to the damping [23]. Among various trilayer structures for spintronic applications, the CoFeB-based soft ferromagnetic thin films have been intensively studied [23, 24]. Recently, proximity-induced magnetization was investigated in Pt/CoFeTaB/Pt trilayer structures, where the degree of polarization in Pt is 10 times higher at Pt/CoFeTaB interfaces than at CoFeTaB/Pt [25].

In this article, we provide a quantitative analysis of magnetic resonance measurements in terms of intrinsic homogeneous and inhomogeneous contributions to the FMR linewidth of model structures of as-deposited and annealed Pt/CoFeTaB/Ir and Ir/CoFeTaB/Pt trilayer structures. These structures have the broken inversion symmetry required for interfacial DMI, and heavy-metal layers which often exhibit PIM. We demonstrate how careful analysis of the angular and temperature dependence of the resonance field and linewidth from FMR enables us to draw conclusions about the differing microstructure in these devices.

EXPERIMENTAL PROCEDURES

In this work, two sets of Pt/CoFeTaB/Ir and Ir/CoFeTaB/Pt trilayer thin films were deposited at room temperature on Si/SiO_2 substrate using dc magnetron sputtering under ultra-high vacuum. In the notation, used in this work, the most left layer corresponds to the bottom layer, while the most right layer is the top one (e.g., the Pt/CoFeTaB/Ir sample has Ir as the cap layer). The capping and buffer layers have a thickness of 3 nm, and the ferromagnetic CoFeTaB layers have a thickness of 10 nm and a composition of $Co_{32}Fe_{32}Ta_{20}B_{16}$, where the numbers in subscript are the atomic percentages.

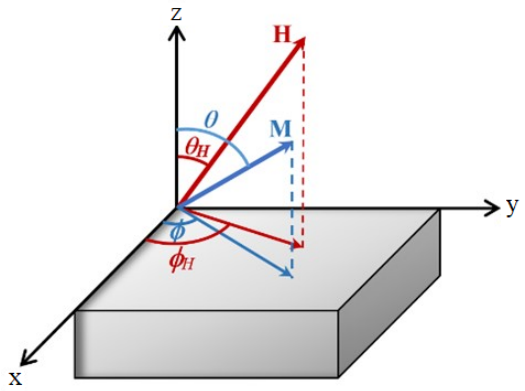

FIG. 1. Used coordinate system on the thin film geometry of the CoFeTaB multilayers and orientations of the magnetic field (H), and magnetization vector (M).

CoFeTaB is an amorphous ferromagnetic alloy where the saturation magnetization and Curie temperature can be tailored by varying the concentration of Ta [25, 26] in the alloy, diluting the magnetic constituents. This composition of CoFeTaB has a nominal Curie temperature of around 115°C. After the deposition, one set of the thin film was annealed at 300°C temperature for one hour to study the influence of annealing treatment on the magnetic properties. Structural characterization by X-ray reflectivity was used to confirm deposition rates and nominal layer thicknesses. Ferromagnetic resonance spectra were recorded with a JOEL X-band electron spin resonance spectrometer which operates at 9.8 GHz frequency at a temperature range between 123 K to room temperature.

THEORETICAL MODEL

The magnetization dynamics of a thin ferromagnetic layer in a hetero-structured system depends on many various parameters, such as thickness, interlayer interaction, interface quality, crystalline and stress-induced magnetic anisotropies, and damping constant. In this study, the magnetization dynamics of the Si/SiO_2/(Ir)Pt/CoFeTaB/(Pt)Ir multilayers have been analyzed by using the FMR spectrometer at different temperatures. The effects of the thermal treatment on the magnetic parameters of the films also have been analyzed with a suitable model which is given in [27–31]. In this model, the polar (θ) and azimuthal (ϕ) coordinates of magnetization and external magnetic field vector are represented in a coordinate system as shown in Fig.1.

In general, the total free energy density (E) for uniform precession of the magnetization in thin film structures contains Zeeman energy in the external dc magnetic field (H), demagnetization energy, contributions due to various terms of crystal magnetic anisotropy (such as the effective perpendicular uniaxial anisotropy, bulk, and strain-induces anisotropy energies). However, we did not observe magneto-crystalline anisotropy in the experimental measurements of angular-dependent FMR spectra in the in-plane geometry, as expected for the thin films of a soft amorphous magnetic material (in our case, it is CoFeTaB). Therefore, the use of only two terms (Zeeman term and combined shape and perpendicular anisotropy term) in the theoretical analysis presented below is adequate:

$$\mathrm{E} = -\,\mathrm{M}_0.\mathrm{H} + (2\pi\mathrm{M}_0^2 - \mathrm{K_p})\cos^2\theta, \tag{1}$$

where M_0 is the saturation magnetization, K_p, is the perpendicular anisotropy constant, and $\cos\theta$ is the polar angle of the magnetization with respect to the normal to the film. Due to the identical symmetry of the shape (demagnetizing) and perpendicular anisotropies, they are usually rewritten to use an effective magnetization as a single parameter using the following relation:

$$4\pi\mathrm{M_{eff}} = 4\pi\mathrm{M}_0 - 2\frac{\mathrm{K_p}}{\mathrm{M}_0} \rightarrow \mathrm{M_{eff}} = \mathrm{M}_0 - \frac{\mathrm{K_p}}{2\pi\mathrm{M}_0}, \tag{2}$$

where $\mathrm{K_p}/2\pi\mathrm{M}_0$ is the perpendicular anisotropy field ($\mathrm{H_p}$). The resonance condition, obtained by a well-known Smit-Beljers-Suhl approach [32] is as follows:

$$\left(\frac{\omega_0}{\gamma}\right)^2 = \mathrm{H}_1 \times \mathrm{H}_2 \tag{3}$$

where ω_0 is the angular resonance frequency, γ is the gyromagnetic ratio. In the case when the magnetic field H is applied at an angle θ_H with respect to the thin film plane normal, the H_1 and H_2 are given by:

$$\begin{aligned} \mathrm{H}_1 &= \mathrm{H_{res}}\cos(\theta_\mathrm{H} - \theta) - 4\pi\mathrm{M_{eff}}\cos 2\theta \\ \mathrm{H}_2 &= \mathrm{H_{res}}\cos(\theta_\mathrm{H} - \theta) - 4\pi\mathrm{M_{eff}}\cos^2\theta \end{aligned} \tag{4}$$

where H_1 and H_2 denote to the anisotropy fields for the out-of-plane geometry. The magnetic damping constant of ferromagnetic thin films is an important parameter for spintronic devices. The magnetization dynamics is usually described by the Landau-Lifshitz-Gilbert equation. The linewidth of FMR spectra provides direct information on effective damping, which consists of intrinsic Gilbert damping and extrinsic relaxation mechanisms. Intrinsic Gilbert damping is related to spin-orbital coupling. In multilayers, an additional contribution to the relaxation appears due to spin-pumping effects. Another extrinsic relaxation mechanism arises due to two-magnon scattering (TMS), representing the process of energy transfer from the uniform precession mode to spin wave modes with the following dissipation to lattice thermal vibration. Finally, we have to consider also inhomogeneous broadening due to the spatial variation of magnetic parameters.

By measuring the angular-dependent FMR, we extracted the extrinsic and intrinsic magnetic damping contributions

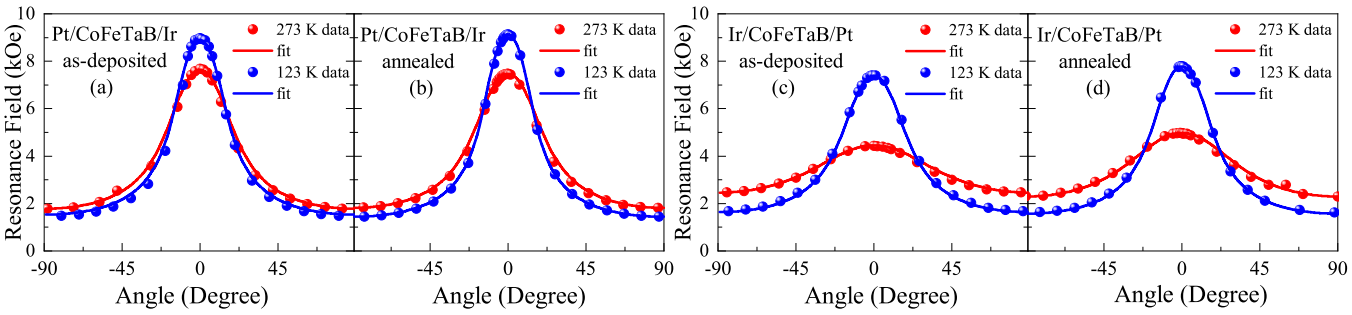

FIG. 2. Measured and fitted out-of-plane angular dependence of resonance field (H_{res}) for as-deposited (a-c) and annealed (b-d) Pt-capped and Ir-capped thin films at 123 K and 273 K. Closed circles represent the experimental data, and the solid lines show the theoretical fitting curves.

of the ferromagnetic CoFeTaB thin film. The peak-to-peak linewidth (ΔH_{pp}) is generally given as:

$$\Delta H_{pp} = \Delta H_{pp}^{\alpha} + \Delta H_{pp}^{inh} + \Delta H_{pp}^{TMS} \quad (5)$$

The first term in the above-given expression for the FMR linewidth is the effective Gilbert damping parameter due to intrinsic damping and additional extrinsic spin-pumping contribution for a given multilayer structure. The second term is the contribution of the inhomogeneity in the magnetization distribution, and the third term is the effect of the two-magnon scattering. The contribution to the peak-to-peak linewidth from effective Gilbert damping is angular dependent and can be written as;

$$\Delta H_{pp}^{\alpha} = \frac{2}{\sqrt{3}} \frac{\omega}{\gamma} \frac{\alpha}{\Xi} \quad (6)$$

where α is the effective Gilbert damping parameter [33], Ξ is the so-called dragging function [31], which enhances the linewidth from the Gilbert damping mechanism, and given by

$$\Xi \equiv \cos(\theta_H - \theta) - \frac{3H_1 + H_2}{H_2(H_1 + H_2)} H_{res} \sin^2(\theta_H - \theta). \quad (7)$$

Thus, the ferromagnetic material intrinsic properties and neighbor material parameters (i.e. spin pumping) define the effective Gilbert damping parameter, α in the first (homogeneous line broadening) term. The inhomogeneous broadening of the experimental peak-to-peak linewidth due to spatial non-uniformity of the magnetic material is also angular dependent, and given by [34]

$$\Delta H_{pp}^{inh} = \frac{1}{\sqrt{3}} \left[\left| \frac{\partial H_{res}}{\partial (M_{eff})} \right| \Delta (M_{eff}) + \left| \frac{\partial H_{res}}{\partial \theta_H} \right| \Delta \theta_H \right], \quad (8)$$

where the first term is the average variation of the effective magnetization over the thin film surface due to the presence of defects, $\Delta(M_{eff})$, and the second term is inhomogeneous broadening due to an angular spread, $\Delta\theta_H$, in the crystallite orientation [35]. The last term in Eq.5 is the contribution of the two-magnon scattering (TMS) induced by surface defects and can be written as [31]

$$\Delta H_{pp}^{TMS} = \frac{2}{\sqrt{3}} \Gamma(H_{res}, \theta_H) \sin^{-1} \sqrt{\frac{H_1}{H_1 + M_{eff}} \frac{\cos 2\theta}{\cos^2 \theta}}, \quad (9)$$

where $\Gamma(H_{res}, \theta_H)$ is the fitting function that changes with the orientation of the external magnetic field (see the details in [31]). Using this described theoretical model, a computer program was written to fit experimental FMR data. The magnetic properties were determined by fitting the theoretical resonance field values to the experimental ones as a function of angle.

RESULTS AND DISCUSSION

The effective magnetization, perpendicular anisotropy, and damping parameters of magnetization have been obtained by analyzing the angular dependent FMR spectra at different temperatures of as-deposited and annealed Pt/CoFeTaB/Ir ('Ir-capped') structure compared with the nominal structural inverse Ir/CoFeTaB/Pt ('Pt-capped') thin films. The out-of-plane angular dependence of the resonance fields (H_{res}) are shown in Fig.2 for as-deposited and annealed Ir-capped and Pt-capped thin films for two different temperatures of 123 K and 273 K (room temperature). In the out-of-plane FMR experiments, the direction of the applied field is rotated in the plane perpendicular to the plane of a thin film sample. Using the resonance conditions given in Eq.3, the experimental data, measured at 273 K and 123 K, have been fitted (shown by the solid lines presented in Fig.2) to determine the magnetic parameters. It should be noted that the values of the perpendicular anisotropy have been extracted as separate parameters because the saturation magnetization values for these samples have been obtained from the vibrating sample magnetometry (VSM) measurements as the secondary technique (the results are not presented in this work and available from corresponding author [supplementary]). A very good agreement has been observed between the measured resonance fields and fits in all cases.

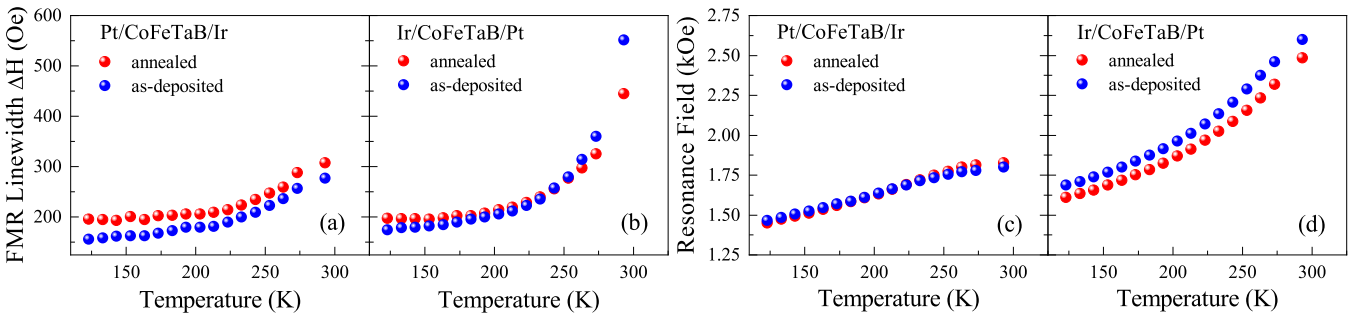

FIG. 3. Temperature dependence of the in-plane FMR linewidth and resonance fields obtained at varying temperatures from 123 K up to room temperature for the un-annealed and annealed thin film structures.

The increase in resonance field as the thin film is rotated such that the applied field is perpendicular to the film plane suggests that the demagnetizing field dominates over any perpendicular magnetic anisotropy, resulting in an easy-plane anisotropy. The simulation results of the angular dependent resonance field (red and blue solid lines in Fig.2) given in Table I, confirm that there is a perpendicular magnetic anisotropy (PMA) contribution to the effective magnetization.

The difference in resonance field between in-plane and perpendicular field orientation scales with the effective magnetization, as described by Eq. 4. Comparing datasets measured at room temperature and 123 K shows that effective magnetization varies strongly with temperature for Pt-capped thin films, and is more weakly temperature dependent for Ir-capped thin films. In all cases the effective magnetization increases as the temperature decreases, confirming that the behavior is dominated by the saturation magnetization rather than the perpendicular magnetic anisotropy term. The perpendicular anisotropy constant is negative for Ir-capped thin films, so favoring in-plane magnetization. This is expected since a CoFeTaB thickness of 10 nm is much greater than the critical thickness where the demagnetization becomes much stronger than the interfacial PMA [10].

The nominal Curie temperature of the CoFeTaB thin film is around 100 K above room temperature. For the Pt-capped thin films, the more strongly temperature-dependent magnetization suggests that the Curie temperature is somewhat reduced to only slightly above room temperature - possibly as a result of diffusion of either Pt or Ir into CoFeTaB, further diluting the magnetic constituents. Since Pt magnetically polarizes strongly [25], this is likely to be a result of Ir diffusion into CoFeTaB during thin film growth. Incorporation of significant amounts of Ir into CoFeTaB results in a positive perpendicular magnetic anisotropy, as is often found in such alloys. In these films, the perpendicular anisotropy is still insufficiently strong to overcome the demagnetizing field, and the thin film remains preferentially magnetized in-plane. As the temperature is reduced the anisotropy becomes slightly negative, preferring in-plane magnetization. The magnetization increases slightly after annealing, accompanied by a reduction in the strength of the perpendicular magnetic anisotropy. This suggests a thermally-driven diffusion of some Ir back out of the CoFeTaB layer.

Fig. 3 shows the temperature dependence of the FMR linewidth [(a) and (b)] and resonance field [(c) and (d)] for measurements taken with the field applied in the plane of the thin film. The resonance fields shift to the lower magnetic field with lowering temperature as the saturation magnetization increases. For Ir-capped thin films, this shift is fairly linear in temperature, suggesting that the Curie temperature is significantly above room temperature, whereas for the Pt-capped thin films, the shift becomes more pronounced at higher temperatures; indicating that the magnetization changes more drastically since the temperature approaches the Curie temperature of these thin films.

The FMR linewidth is a measure of the relaxation rate of the magnetization and provides a convenient way to measure the magnetic damping parameters. As seen in Fig.3(a) and (b), the FMR linewidths are roughly independent of temperature below around 230 K, and above this temperature, they increase; slowly for Ir-capped films but more strongly for Pt-capped films - again possibly as a result of the closer proximity to the Curie temperature in the Pt-capped films.

The effective magnetization is calculated by using Eq. 2 then the effective Gilbert damping parameter, α, is calculated by fitting Eq. 6. The α value for the as-deposited Ir-capped thin film at room temperature is 0.054. This relatively high value for the effective damping is due to a combination of relatively high intrinsic damping in CoFeTaB, which may be anticipated as a result of the strong spin-orbit coupling in Ta, and a contribution from spin-pumping into both the Ir capping layer and Pt underlayer. Annealing the Ir-capped structure results in a slight increase in the effective damping to 0.064 at room temperature. This may again be indicative of some incorporation of strongly-spin-orbit-coupled Ir into the CoFeTaB layer during annealing. In both cases the damping reduces slightly as temperature decreases; this is consistent with a decrease in the spin-pumping contribution to the effective damping as the spin-diffusion length in Pt and/or Ir increases with reducing temperature [6].

The angular dependence of the peak-to-peak linewidth, ΔH, as the applied field is rotated out of the plane is shown in Fig.4. An important feature shown here is that, for the Ir-capped thin film, the linewidth in the perpendicular geome-

		Pt/CoFeTaB/Ir as-deposited		Pt/CoFeTaB/Ir annealed		Ir/CoFeTaB/Pt as-deposited		Ir/CoFeTaB/Pt annealed	
		273 K	**123 K**	**273 K**	**123 K**	**273 K**	**123 K**	**273 K**	**123 K**
M_0	(emu/cm^3)	-	677	-	550	-	1523	-	1194
M_{eff}	(emu/cm^3)	350	450	345	468	110	340	150	370
H_p	(Oe)	-	227	-	82	-	1183	-	824
ΔH_{pp}^{TMS}	(Oe)	120	50	100	60	-	40	-	30
$\Delta\theta_H$	(degree)	-	-	-	-	0.02	0.02	0.012	-
$\Delta(M_{eff})$	(emu/cm^3)	-	-	-	-	100	-	100	-
α		0.054	0.039	0.064	0.047	0.1	0.1	0.087	0.05

TABLE I. Deduced magnetic parameters of the thin film structures. The g-factor is 2.2 for all thin films. The error bars of the values given are of the order of 5%.

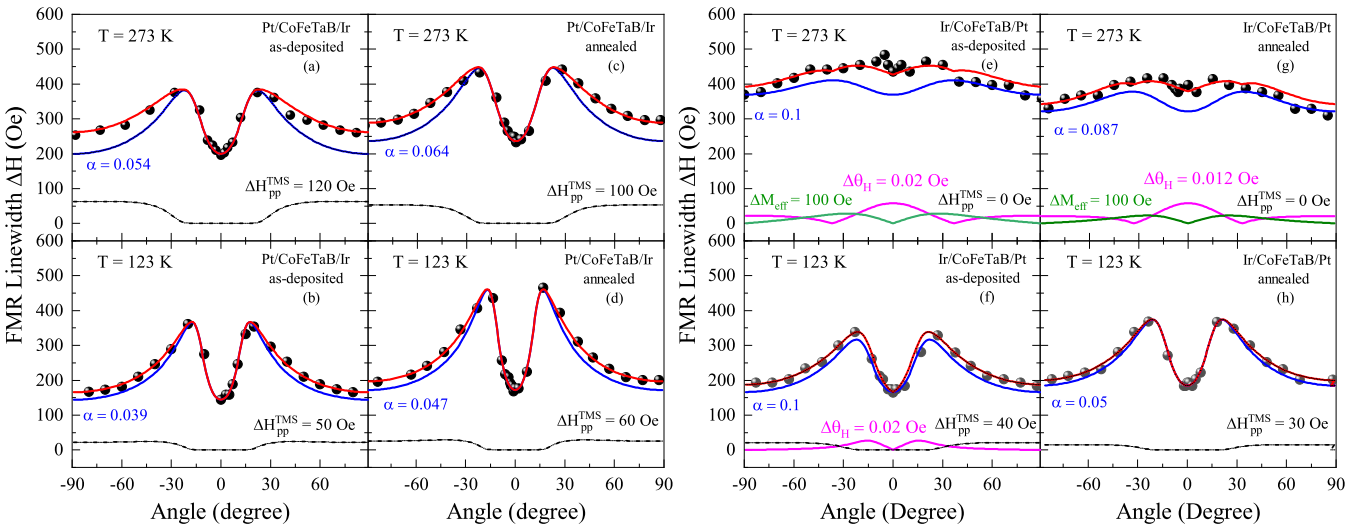

FIG. 4. Measured and fitted out-of-plane angular dependence of FMR linewidths ΔH_{pp} for as-deposited and annealed Pt-capped and Ir-capped thin films at 123 K and 273 K. Closed circles represent the experimental data, and the solid lines show the theoretical fitting curves.

try ($\theta_H = 0$) is clearly smaller than that for the in-plane geometry ($\theta_H = 90$). This indicates that there is a contribution to the damping due to the two-magnon scattering (TMS) mechanism. Values extracted from fitting the angular dependence of resonance frequency and linewidth are shown in Table I. Several explanations can be suggested as to the origin of the variations in magnetization, anisotropy, and damping behavior on annealing; such as modifications of the surface/interface roughness, interdiffusion and mixing, and interfacial hybridization between the ferromagnet and adjacent layers. All these are frequently found to be modified by annealing.

For both un-annealed and annealed Ir-capped thin films, the TMS contribution to the linewidth decreases as the temperature decreases; with the decrease in TMS contribution being greater for the un-annealed thin film. This suggests that annealing acts to modify the structure at the Pt/CoFeTaB interface. This is consistent with the increase in effective Gilbert damping due to enhanced spin-pumping across an improved interface. These thin films show a negligible contribution from the inhomogeneous damping, demonstrating that the magnetization and magnetic anisotropy are uniform within the amorphous ferromagnetic layer.

For as-deposited Pt-capped thin films at room temperature, due to the large amount of Ir diffusion into the ferromagnetic layer, the effective Gilbert damping, α, is around 0.1 and there is a contribution due to the magnetic inhomogeneity, primarily in the magnitude of the effective magnetization; suggesting the Ir is not uniformly distributed through the layer. The interface structure is more uniform and the angular dependency of FMR linewidth at room temperature indicates an absence of TMS. At lower temperatures, there is an additional contribution to the damping from TMS, a reduction in the contributions from inhomogeneous damping, with the magnetization becoming more spatially uniform, and surprisingly there is no change in the effective Gilbert damping. After annealing, the damping parameter reduces slightly at room temperature, again consistent with a thermally-driven removal of some Ir from the CoFeTaB layer. There is a similar contribution from magnetic inhomogeneity and no TMS at room temperature. At lower temperatures the TMS mechanism again becomes active, and the inhomogeneous damping contributions become negligible. The effective Gilbert damping again reduces as the temperature is reduced, similar to the case for

Ir-capped structures.

For the Ir-capped thin films, there is a relatively small difference between the magnetic parameters of un-annealed and annealed thin films in comparison to the differences between un-annealed and annealed Pt-capped thin films. The effective magnetization of Pt-capped films is much lower than for the Ir-capped films at room temperature. This is attributed to Ir diffusion into the ferromagnetic CoFeTaB layer during the deposition process. This Ir incorporation reduces the Curie temperature and enhances both the effective Gilbert damping and the perpendicular magnetic anisotropy constant.

CONCLUSIONS

In this work, the ferromagnetic resonance study of the magnetic properties of Pt/CoFeTaB/Ir and Ir/CoFeTaB/Pt trilayer thin films has been presented. Analysis of angular and temperature dependent FMR spectra revealed significant differences in their magnetic behavior depending on the deposition order in the magnetic trilayer thin films. The detailed analysis of the angular dependent FMR spectra allows us to separate various contributions in the linewidth, such as the homogeneous broadening due to effective Gilbert damping (including spin pumping effect), conventional inhomogeneous broadening (non-uniformity in the magnetic properties), and two-magnon-scattering (TMS) contributions to the magnetic dissipation. For the Pt/CoFeTaB/Ir sample (i.e., the Ir-capped multilayer) the static and dynamic magnetic behaviors have weaker dependence on temperature and they are not modified essentially by annealing. However, for the Ir/CoFeTaB/Pt (the Pt-capped multilayer), which differs only by reversal of the deposition order, the essential effect of temperature and annealing on the magnetic properties have been observed. For the Pt-capped sample, significant incorporation of Ir into the CoFeTaB layer is anticipated. The apparent effect of annealing is attributed to the decrease in the Ir concentration within the ferromagnetic layer in the annealed sample. A strong asymmetry in various broadening contributions between two kinds of the studied multilayers supports this picture. For instance, strong TMS contribution to FMR linewidth at room temperature has been observed only in the Ir-capped thin films. Thus, the analysis of temperature and angular dependences of the FMR signals has revealed rather detailed information on the microscale structure of the magnetic trilayers studied in this work.

DECLARATIONS

Ethical Approval
Not applicable

Competing Interests
The authors have no competing interests as defined by Springer, or other interests that might be perceived to influence the results and/or discussion reported in this article.

Authors' Contributions
B. Ö., N. A., and B. N. performed experiments, and M. T., S. K., B. R., and A. T. H. wrote the main manuscript text. All authors reviewed the manuscript.

Funding
B. N. is grateful to EPSRC for the provision of a DTP studentship. A. T. H. acknowledges financial support from the Royal Society.

Availability of Data and Materials
The datasets generated during and/or analyzed during the current study are available from the corresponding author upon reasonable request.

* email: kazan@gtu.edu.tr

[1] L. Zhu, D. C. Ralph, and R. A. Buhrman, Effective spin-mixing conductance of heavy-metal–ferromagnet interfaces, Physical Review Letters **123**, 057203 (2019).
[2] W. Zhang, V. Vlaminck, J. E. Pearson, R. Divan, S. D. Bader, and A. Hoffmann, Determination of the pt spin diffusion length by spin-pumping and spin hall effect, Applied physics letters **103**, 242414 (2013).
[3] V. Vlaminck, J. E. Pearson, S. D. Bader, and A. Hoffmann, Dependence of spin-pumping spin hall effect measurements on layer thicknesses and stacking order, Physical Review B **88**, 064414 (2013).
[4] O. Mosendz, J. Pearson, F. Fradin, G. Bauer, S. Bader, and A. Hoffmann, Quantifying spin hall angles from spin pumping: Experiments and theory, Physical review letters **104**, 046601 (2010).
[5] H. Nakayama, M. Althammer, Y.-T. Chen, K.-i. Uchida, Y. Kajiwara, D. Kikuchi, T. Ohtani, S. Geprägs, M. Opel, S. Takahashi, *et al.*, Spin hall magnetoresistance induced by a nonequilibrium proximity effect, Physical review letters **110**, 206601 (2013).
[6] S. Marmion, M. Ali, M. McLaren, D. Williams, and B. Hickey, Temperature dependence of spin hall magnetoresistance in thin yig/pt films, Physical Review B **89**, 220404 (2014).
[7] A. W. Wells, P. M. Shepley, C. H. Marrows, and T. A. Moore, Effect of interfacial intermixing on the dzyaloshinskii-moriya interaction in pt/co/pt, Physical review B **95**, 054428 (2017).
[8] D. Meier, D. Reinhardt, M. Van Straaten, C. Klewe, M. Althammer, M. Schreier, S. T. Goennenwein, A. Gupta, M. Schmid, C. H. Back, *et al.*, Longitudinal spin seebeck effect contribution in transverse spin seebeck effect experiments in pt/yig and pt/nfo, Nature communications **6**, 8211 (2015).
[9] C. Deger, Strain-enhanced dzyaloshinskii–moriya interaction at co/pt interfaces, Scientific Reports **10**, 1 (2020).
[10] A. Hrabec, N. Porter, A. Wells, M. Benitez, G. Burnell, S. McVitie, D. McGrouther, T. Moore, and C. Marrows, Measuring and tailoring the dzyaloshinskii-moriya interaction in perpendicularly magnetized thin films, Physical Review B **90**, 020402 (2014).
[11] M. Tokaç, S. Bunyaev, G. Kakazei, D. Schmool, D. Atkinson,

and A. Hindmarch, Interfacial structure dependent spin mixing conductance in cobalt thin films, Physical review letters **115**, 056601 (2015).

[12] T. Fache, J. Rojas-Sanchez, L. Badie, S. Mangin, and S. Petit-Watelot, Determination of spin hall angle, spin mixing conductance, and spin diffusion length in cofeb/ir for spin-orbitronic devices, Physical Review B **102**, 064425 (2020).

[13] A. Belabbes, G. Bihlmayer, F. Bechstedt, S. Blügel, and A. Manchon, Hund's rule-driven dzyaloshinskii-moriya interaction at 3d-5d interfaces., Physical review letters **117 24**, 247202 (2016).

[14] X. Ma, G. Yu, C. Tang, X. Li, C. He, J. Shi, K. L. Wang, and X. Li, Interfacial dzyaloshinskii-moriya interaction: effect of 5 d band filling and correlation with spin mixing conductance, Physical review letters **120**, 157204 (2018).

[15] S. Tacchi, R. Troncoso, M. Ahlberg, G. Gubbiotti, M. Madami, J. Åkerman, and P. Landeros, Interfacial dzyaloshinskii-moriya interaction in pt/cofeb films: effect of the heavy-metal thickness, Physical review letters **118**, 147201 (2017).

[16] N.-H. Kim, J. Jung, J. Cho, D.-S. Han, Y. Yin, J.-S. Kim, H. J. Swagten, and C.-Y. You, Interfacial dzyaloshinskii-moriya interaction, surface anisotropy energy, and spin pumping at spin orbit coupled ir/co interface, Applied physics letters **108**, 142406 (2016).

[17] J. Geissler, E. Goering, M. Justen, F. Weigand, G. Schütz, J. Langer, D. Schmitz, H. Maletta, and R. Mattheis, Pt magnetization profile in a pt/co bilayer studied by resonant magnetic x-ray reflectometry, Physical Review B **65**, 020405 (2001).

[18] K. Gupta, R. J. Wesselink, R. Liu, Z. Yuan, and P. J. Kelly, Disorder dependence of interface spin memory loss, Physical review letters **124**, 087702 (2020).

[19] S.-Y. Huang, X. Fan, D. Qu, Y. Chen, W. Wang, J. Wu, T. Chen, J. Xiao, and C. Chien, Transport magnetic proximity effects in platinum, Physical review letters **109**, 107204 (2012).

[20] M. Caminale, A. Ghosh, S. Auffret, U. Ebels, K. Ollefs, F. Wilhelm, A. Rogalev, and W. Bailey, Spin pumping damping and magnetic proximity effect in pd and pt spin-sink layers, Physical Review B **94**, 014414 (2016).

[21] K.-S. Ryu, S.-H. Yang, L. Thomas, and S. S. Parkin, Chiral spin torque arising from proximity-induced magnetization, Nature communications **5**, 3910 (2014).

[22] H. Yang, A. Thiaville, S. Rohart, A. Fert, and M. Chshiev, Anatomy of dzyaloshinskii-moriya interaction at co/pt interfaces, Physical review letters **115**, 267210 (2015).

[23] M. Belmeguenai, D. Apalkov, M. Gabor, F. Zighem, G. Feng, and G. Tang, Magnetic anisotropy and damping constant in cofeb/ir and cofeb/ru systems, IEEE Transactions on Magnetics **54**, 1 (2018).

[24] W. Skowroński, T. Nozaki, Y. Shiota, S. Tamaru, K. Yakushiji, H. Kubota, A. Fukushima, S. Yuasa, and Y. Suzuki, Perpendicular magnetic anisotropy of ir/cofeb/mgo trilayer system tuned by electric fields, Applied Physics Express **8**, 053003 (2015).

[25] O. Inyang, L. Bouchenoire, B. Nicholson, M. Tokaç, R. Rowan-Robinson, C. Kinane, and A. Hindmarch, Threshold interface magnetization required to induce magnetic proximity effect, Physical Review B **100**, 174418 (2019).

[26] M. Tokaç, C. J. Kinane, D. Atkinson, and A. T. Hindmarch, Temperature dependence of magnetically dead layers in ferromagnetic thin-films, AIP Advances **7**, 10.1063/1.4997366 (2017), 115022.

[27] S. Kazan, B. Kocaman, A. Parabaş, and F. Yıldız, Collective spin behavior of nige thin films on mgo substrate, Journal of Magnetism and Magnetic Materials **527**, 167722 (2021).

[28] R. Topkaya, S. Kazan, R. Yilgin, N. Akdoğan, M. Özdemir, and B. Aktaş, Ferromagnetic resonance studies of exchange biased coo/fe bilayer grown on mgo substrate, Journal of Superconductivity and Novel Magnetism **27**, 1503 (2014).

[29] R. Yilgin, M. Oogane, S. Yakata, Y. Ando, and T. Miyazaki, Intrinsic gilbert damping constant in co/sub 2/mnal heusler alloy films, IEEE transactions on magnetics **41**, 2799 (2005).

[30] H. Sakimura, A. Asami, T. Harumoto, Y. Nakamura, J. Shi, and K. Ando, Enhancement of two-magnon scattering induced by a randomly distributed antiferromagnetic exchange field, Physical Review B **98**, 144406 (2018).

[31] J. Lindner, I. Barsukov, C. Raeder, C. Hassel, O. Posth, R. Meckenstock, P. Landeros, and D. Mills, Two-magnon damping in thin films in case of canted magnetization: Theory versus experiment, Physical Review B **80**, 224421 (2009).

[32] H. Beljers and J. Smit, Ferromagnetic resonance absorption in bafe12o19 a highly anisotropic crystal, Phil. Res. Rep **10** (1955).

[33] T. L. Gilbert, A phenomenological theory of damping in ferromagnetic materials, IEEE transactions on magnetics **40**, 3443 (2004).

[34] M. Oogane, T. Wakitani, S. Yakata, R. Yilgin, Y. Ando, A. Sakuma, and T. Miyazaki, Magnetic damping in ferromagnetic thin films, Japanese journal of applied physics **45**, 3889 (2006).

[35] S. Mizukami, Y. Ando, and T. Miyazaki, Effect of spin diffusion on gilbert damping for a very thin permalloy layer in cu/permalloy/cu/pt films, Physical Review B **66**, 104413 (2002).